

Institute for Advanced Simulation

Bond-Order Potentials for Bridging the Electronic to Atomistic Modelling Hierarchies

Thomas Hammerschmidt and Ralf Drautz

published in

Multiscale Simulation Methods in Molecular Sciences,
J. Grotendorst, N. Attig, S. Blügel, D. Marx (Eds.),
Institute for Advanced Simulation, Forschungszentrum Jülich,
NIC Series, Vol. 42, ISBN 978-3-9810843-8-2, pp. 229-246, 2009.

© 2009 by John von Neumann Institute for Computing
Permission to make digital or hard copies of portions of this work for
personal or classroom use is granted provided that the copies are not
made or distributed for profit or commercial advantage and that copies
bear this notice and the full citation on the first page. To copy otherwise
requires prior specific permission by the publisher mentioned above.

<http://www.fz-juelich.de/nic-series/volume42>

Bond-Order Potentials for Bridging the Electronic to Atomistic Modelling Hierarchies

Thomas Hammerschmidt and Ralf Drautz

Interdisciplinary Centre for Advanced Materials Simulation (ICAMS)
Ruhr-Universität Bochum
Stiepeler Strasse 129, 44801 Bochum, Germany
E-mail: {thomas.hammerschmidt, ralf.drautz}@rub.de

Robust interatomic potentials must be able to describe the making and breaking of interatomic bonds in a computationally efficient format so that the potentials may be employed in large-scale atomistic simulations. We summarize the fundamentals of such potentials, the bond-order potentials, and their derivation from the electronic structure. By coarse graining the tight-binding electronic structure and relating it to the local atomic environment, the bond-order potentials are derived as quantum-mechanical footed effective interatomic interactions.

1 What are Bond-Order Potentials?

Bond-order potentials are interatomic potentials that are derived from quantum mechanics. In contrast to classical empirical potentials, bond-order potentials capture bond formation and breaking, saturated and unsaturated bonds, dangling bonds and radical bonds, as well as single, double or triple bonds. The bond-order potentials provide similar accuracy as tight-binding calculations at less computational effort, and thus open the way to large-scale atomistic simulations of systems which cannot be described by classical empirical potentials.

The bond-order potentials (BOPs) are derived by systematically coarse graining the electronic structure at two levels of approximation,

1. In the first step, the density functional theory (DFT) formalism is approximated in terms of physically and chemically intuitive contributions within the tight-binding (TB) bond model^{1,2}. The TB approximation is sufficiently accurate to predict structural trends across the sp-valent and d-valent elements, as well as sufficiently simple to allow a physically meaningful interpretation of the bonding in terms of σ , π and δ contributions. The parameters of the TB model can be obtained from ab-initio calculations in a systematic way.
2. In the second step, the TB electronic structure is coarse grained and related to the local topology and coordination of the material. The functional form of the bond energy is derived as a function of the positions and the types of atoms that surround a given bond.

The first step of coarse graining from DFT to TB is discussed by Anthony Paxton in his contribution to this issue¹. In this contribution we will start from the TB description of the electronic structure, focus on the second level of coarse graining and discuss how the electronic structure may be hidden in effective interatomic interactions.

1.1 Aim of this Contribution and some Literature

With this short introduction we do not aim at giving an overview of the bond-order potentials. Instead, with our contribution we would like to give an easy to read summary of the ideas and concepts that are used to coarse grain the electronic structure into effective interatomic interactions. A recent special issue *Modelling Electrons and Atoms for Materials Science* of Progress in Materials Science³ contains a number of reviews that give a detailed overview of the bond-order potentials and their application to the simulation of elastic and plastic properties of transition metals, the growth of semiconductor thin films and hydrocarbons⁴⁻⁷. We would like to recommend these reviews to the interested reader.

2 Binding Energy

The starting point for the derivation of bond-order potentials is the tight-binding bond model² that is introduced in the lecture of Anthony Paxton¹. The binding energy within the tight-binding bond model is given as the sum of covalent bond energy U_{bond} , promotion energy U_{prom} , and repulsive energy U_{rep} ,

$$U_B = U_{\text{bond}} + U_{\text{prom}} + U_{\text{rep}}. \quad (1)$$

The promotion energy is calculated as a sum over orbitals $|i\alpha\rangle$ centred on atom i (where α labels the valence orbital), whereas the repulsive energy is often approximated as sum over pairs of atoms

$$U_{\text{prom}} = \sum_{i\alpha} E_{i\alpha}^{(0)} \left(N_{i\alpha} - N_{i\alpha}^{(0)} \right), \quad (2)$$

$$U_{\text{rep}} = \sum_{ij} \phi_{ij} (R_{ij}), \quad (3)$$

with the free atom reference onsite levels $E_{i\alpha}^{(0)}$. The promotion energy accounts for the redistribution of the electrons across the orbitals of an atom due to hybridisation. The simplest form of the repulsive energy as given above is a pairwise term that depends solely on the interatomic distance R_{ij} between atoms i and j . Some materials require a more complex description of the repulsive energy, *e.g.* Mrovec *et al.*⁸ introduced a Yukawa-type environment-dependent term to account for the strong core repulsion in transition metals.

As we will see in the following, the bond energy U_{bond} can be given in either onsite representation (in terms of the atom-based density of states) or intersite representation (in terms of the bond-based density matrix or bond order). The two representations are equivalent but offer different views on the formation of bonds in materials.

2.1 Bond Energy: Onsite Representation

The onsite representation of the bond energy is based on the local density of states $n_{i\alpha}(E)$ of orbital α on atom i . The contribution of each orbital to the bond energy is calculated by integrating its local density of states (DOS) up to the Fermi level E_F

$$U_{\text{bond}} = 2 \sum_{i\alpha} \int_{E_F} (E - E_{i\alpha}) n_{i\alpha}(E) dE. \quad (4)$$

The factor of two accounts for the neglect of magnetism in the model, so that spin up and spin down spin channels are degenerate. The onsite level $E_{i\alpha}$ is shifted relative to its free atom value $E_{i\alpha}^{(0)}$ until self-consistency is achieved (cf. lecture of Anthony Paxton¹). The local density of states $n_{i\alpha}(E)$ may be obtained from the eigenfunctions $|\psi_n\rangle$ of the Hamiltonian \hat{H} ,

$$\hat{H}\psi_n = E_n\psi_n, \quad (5)$$

by expressing the eigenfunctions $|\psi_n\rangle$ in an orthonormal basis centred on atoms i

$$|\psi_n\rangle = \sum_{i\alpha} c_{i\alpha}^{(n)} |i\alpha\rangle, \quad (6)$$

where the index α denotes the valence orbital. Then, by calculating the band energy U_{band} as the sum over all occupied orbitals, we find that

$$\begin{aligned} U_{\text{band}} &= 2 \sum_n^{\text{occ}} E_n = 2 \sum_n^{\text{occ}} \langle \psi_n | \hat{H} | \psi_n \rangle = 2 \sum_n^{\text{occ}} E_n \langle \psi_n | \psi_n \rangle \\ &= 2 \sum_n^{\text{occ}} \sum_{i\alpha} \sum_{j\beta} E_n c_{i\alpha}^{*(n)} c_{j\beta}^{(n)} \langle i\alpha | j\beta \rangle = 2 \sum_n^{\text{occ}} \sum_{i\alpha} \sum_{j\beta} E_n c_{i\alpha}^{*(n)} c_{j\beta}^{(n)} \delta_{i\alpha j\beta} \\ &= 2 \sum_{i\alpha} \int_{E_F}^E E \sum_n n_{i\alpha}(E) c_{i\alpha}^{*(n)} c_{i\alpha}^{(n)} dE. \end{aligned} \quad (7)$$

We identify the local density of states of orbital $|i\alpha\rangle$ as

$$n_{i\alpha} = \sum_n \left| c_{i\alpha}^{(n)} \right|^2 \delta(E - E_n), \quad (8)$$

such that the band energy U_{band} is written as

$$U_{\text{band}} = 2 \sum_{i\alpha} \int_{E_F}^E E n_{i\alpha}(E) dE. \quad (9)$$

The bond energy Eq.(4) is the band energy calculated with respect to the onsite levels $E_{i\alpha}$,

$$U_{\text{bond}} = 2 \sum_{i\alpha} \int_{E_F}^E (E - E_{i\alpha}) n_{i\alpha}(E) dE = U_{\text{band}} - \sum_{i\alpha} E_{i\alpha} N_{i\alpha}, \quad (10)$$

with the number of electrons $N_{i\alpha}$ in orbital $|i\alpha\rangle$,

$$N_{i\alpha} = 2 \sum_{i\alpha} \int_{E_F}^E n_{i\alpha}(E) dE. \quad (11)$$

Some authors prefer not to calculate the *bond* energy that is calculated with respect to the onsite levels but to use the *band* energy instead, such that

$$U_B = U_{\text{band}} + U_{\text{prom}} + U_{\text{rep}}. \quad (12)$$

However, as discussed in the lecture of Anthony Paxton¹, this tight-binding *band* model is inconsistent with the force theorem^{2,9,10} while the bond energy in the tight-binding *bond* model properly accounts for the redistribution of charge due to the shift of the onsite levels that arise from atomic displacements.

2.2 Bond Energy: Intersite Representation

An alternative but equivalent representation to the onsite representation of the band energy Eq.(9) is the intersite representation. The intersite representation is obtained by expanding the eigenfunctions $|\psi_n\rangle = \sum_{i\alpha} c_{i\alpha}^{(n)} |i\alpha\rangle$ in terms of the TB basis,

$$\begin{aligned} U_{\text{band}} &= 2 \sum_n^{\text{occ}} E_n = 2 \sum_n^{\text{occ}} \langle \psi_n | \hat{H} | \psi_n \rangle = 2 \sum_{i\alpha} \sum_{j\beta}^{\text{occ}} \sum_n^{\text{occ}} c_{i\alpha}^{*(n)} c_{j\beta}^{(n)} \langle i\alpha | \hat{H} | j\beta \rangle \\ &= 2 \sum_{i\alpha j\beta} \rho_{i\alpha j\beta} H_{i\alpha j\beta}, \end{aligned} \quad (13)$$

with the density matrix

$$\rho_{i\alpha j\beta} = \sum_n^{\text{occ}} c_{i\alpha}^{*(n)} c_{j\beta}^{(n)}. \quad (14)$$

The *bond* energy is obtained from the *band* energy in intersite representation by restricting the summation to off-diagonal elements as $N_{i\alpha} = \rho_{i\alpha i\alpha}$. Therefore, the bond energy in intersite representation is given by

$$U_{\text{bond}} = 2 \sum_{i\alpha \neq j\beta} \rho_{i\alpha j\beta} H_{i\alpha j\beta}. \quad (15)$$

The bond order $\Theta_{i\alpha j\beta}$ of a bond between the valence orbitals α and β of two atoms i and j is just two times the corresponding element of the density matrix

$$\Theta_{i\alpha j\beta} = 2 \rho_{i\alpha j\beta}. \quad (16)$$

By construction the onsite and intersite representation of the bond energy are equivalent

$$U_{\text{bond}} = 2 \sum_{i\alpha} \int_{E_{\text{F}}}^{\text{E}_F} (E - E_{i\alpha}) n_{i\alpha}(E) dE = \sum_{i\alpha \neq j\beta} \Theta_{i\alpha j\beta} H_{i\alpha j\beta}, \quad (17)$$

however, the two representations offer different views on bond formation. We see that while the bond energy in onsite representation is obtained by filling electrons into the local density of states $n_{i\alpha}(E)$ on each atom, the intersite representation calculates the bond energy as a sum over pairwise Hamiltonian matrix elements $H_{i\alpha j\beta}$ that are weighted with the density matrix element $\rho_{i\alpha j\beta}$. In the following we will discuss some properties of the density matrix.

3 Properties of the Bond Order

In the previous section we decomposed *global* quantities, like the bond energy or the band energy, in their *local* contributions, the atom-based local density of states in the onsite representation and the bond-based bond order in the intersite representation. In the following we will discuss some properties of the bond order, while the properties of the local density of states will be discussed in section 4.

An intuitive physical interpretation of the bond order becomes apparent when we transform the atomic orbitals to linear combinations (dimer orbitals)

$$|+\rangle = \frac{1}{\sqrt{2}} (|i\alpha\rangle + |j\beta\rangle) \quad \text{bonding ,} \quad (18)$$

$$|-\rangle = \frac{1}{\sqrt{2}} (|i\alpha\rangle - |j\beta\rangle) \quad \text{antibonding .} \quad (19)$$

The number of electrons in the bonding and antibonding dimer orbitals may be obtained by projection on the occupied eigenstates,

$$N_+ = 2 \sum_n^{\text{occ}} |\langle + | \psi_n \rangle|^2, \quad N_- = 2 \sum_n^{\text{occ}} |\langle - | \psi_n \rangle|^2, \quad (20)$$

By expanding the eigenstates in the atomic basis, Eq.(6), and by making use of the definition of the bond order Eq.(16), one finds that the bond order is one-half the difference between the number of electrons in the bonding state compared to the antibonding state

$$\Theta_{i\alpha j\beta} = \frac{1}{2} (N_+ - N_-) . \quad (21)$$

With a maximum of two electrons in an orbital, the bond order takes its largest absolute value of 1 for two electrons of opposite spin in the bonding and none in the antibonding orbital. Furthermore, as the number of electrons in the bonding state N_+ is less or equal to the total number of electrons in the bond $N_{i\alpha j\beta} = \frac{1}{2} (N_{i\alpha} + N_{j\beta}) = \frac{1}{2} (N_+ + N_-)$,

$$N_+ \leq N_+ + N_-, \quad (22)$$

the value of the bond order in general is limited by an envelope function¹¹

$$|\Theta_{i\alpha j\beta}| \leq \begin{cases} N_{i\alpha j\beta} & \text{for } 0 \leq N_{i\alpha j\beta} \leq 1, \\ 2 - N_{i\alpha j\beta} & \text{for } 1 < N_{i\alpha j\beta} \leq 2 . \end{cases} \quad (23)$$

As an example, consider the H_2 molecule with one s -orbital on each atom. The eigenstates of the H_2 dimer are given by bonding and antibonding linear combinations of the s -orbitals. Both valence electrons occupy the bonding state, while the antibonding state remains empty. Therefore we expect that the H_2 dimer forms a fully saturated covalent bond with bond order $\Theta = 1$. If we look at a He_2 dimer instead, the eigenstates are also given by bonding and antibonding linear combinations of the s -orbitals just like in the case of H_2 . However, now the 4 valence electrons have to completely fill both, the bonding and the antibonding states such that the bond order is zero $\Theta = 0$. Therefore, we expect that the He_2 molecule does not form a covalent bond. In contrast to these two extremal cases, the bond order usually takes intermediate values (see Fig. 1) that depend sensitively on local coordination and number of valence electrons. It is the aim of the bond-order potentials to describe these intermediate values as accurately as possible. More examples and a detailed discussion of the bond order of different molecules and solids is given in the textbook of Pettifor¹².

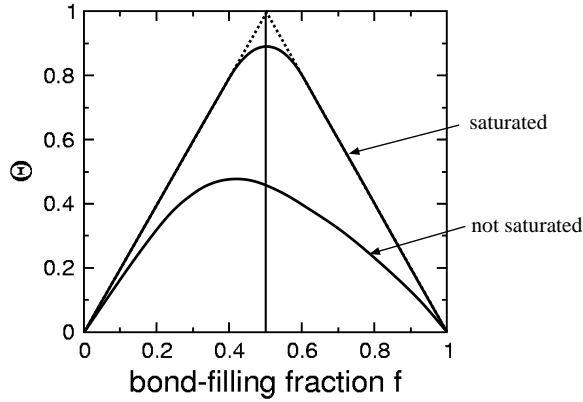


Figure 1. Schematic of the bond order as a function of the number of electrons in the bond (bond-filling fraction $f = N_{i\alpha j\beta}/2$). The bond order of a saturated bond closely follows the envelope function Eq.(23) and is close to 1 at half-full band. Typically materials with open structures like, for example, Si in the diamond lattice, show the formation of saturated bonds. In close-packed crystals, for example in d -valent transition metals, the electrons cannot be distributed only into bonding states, the bonds are not saturated and the bond order takes a smaller value.

4 Moments

For the development of effective interatomic potentials we would like to bypass the numerical diagonalisation of the TB Hamiltonian \hat{H} and instead determine local quantities like the local density of states $n_{i\alpha}(E)$ or the bond order $\Theta_{i\alpha j\beta}$ directly from the local atomic environment. This may be achieved by making use of the moments theorem¹³ that relates the electronic structure $(n_{i\alpha}(E), \rho_{i\alpha j\beta})$ to the crystal structure (the position of the atoms). The N th moment of orbital $|i\alpha\rangle$ is given by

$$\mu_{i\alpha}^{(N)} = \int E^N n_{i\alpha}(E) dE. \quad (24)$$

Inserting the density of states from Eq.(8) and making use of the identity operator

$$\hat{1} = \sum_n |\psi_n\rangle\langle\psi_n|, \quad (25)$$

results in an expression for the moments in terms of atomic orbitals $|i\alpha\rangle$ and the Hamiltonian \hat{H} :

$$\begin{aligned} \mu_{i\alpha}^{(N)} &= \int E^N \sum_n |c_{i\alpha}^{(n)}|^2 \delta(E - E_n) dE \\ &= \sum_n |\langle i\alpha | \psi_n \rangle|^2 E_n^N \\ &= \sum_n \langle i\alpha | \hat{H}^N | \psi_n \rangle \langle \psi_n | i\alpha \rangle \\ &= \langle i\alpha | \hat{H}^N | i\alpha \rangle. \end{aligned} \quad (26)$$

By using an orthogonal basis set that completely spans the TB Hilbert space, *i.e.*

$$\hat{1} = \sum_{j\beta} |j\beta\rangle\langle j\beta|, \quad (27)$$

the N th power of the Hamilton operator acting on orbital $|i\alpha\rangle$ can be written as the product of N Hamilton matrices,

$$\langle i\alpha | \hat{H}^N | i\alpha \rangle = \sum_{j\beta k\gamma \dots} \langle i\alpha | \hat{H} | j\beta \rangle \langle j\beta | \hat{H} | k\gamma \rangle \langle k\gamma | \hat{H} | \dots \rangle \dots \langle \dots | \hat{H} | i\alpha \rangle. \quad (28)$$

Each Hamiltonian matrix element $H_{i\alpha j\beta} = \langle i\alpha | \hat{H} | j\beta \rangle$ connects two neighbouring atoms i and j and is frequently called a *hop*. Looking at the indices, we see that the product of Hamiltonian matrices defines a path through the atomic structure ($|i\alpha\rangle \rightarrow |j\beta\rangle \rightarrow |k\gamma\rangle \rightarrow \dots \rightarrow |i\alpha\rangle$) which we will refer to as hopping path. Therefore the N th moment $\mu_{i\alpha}^{(N)}$, Eq.(26), can be understood as the sum over all hopping paths of length N that start and end on the same orbital $|i\alpha\rangle$,

$$\mu_{i\alpha}^{(N)} = \int E^N n_{i\alpha}(E) dE = \sum_{j\beta k\gamma \dots} H_{i\alpha j\beta} H_{j\beta k\gamma} H_{k\gamma \dots} \dots H_{\dots i\alpha}. \quad (29)$$

Figure 2 illustrates one hopping path that contributes to the 4th moment. As different crystal structures have different numbers of hopping paths of a given lengths, the moments are sensitive to changes in the crystal structure. Higher moments correspond to longer hopping paths and thus to a more far-sighted sampling of the atomic environment.

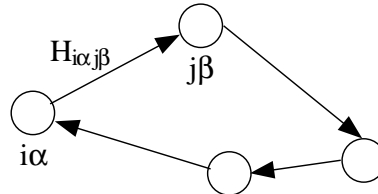


Figure 2. A path that contributes to the 4th moment of orbital $i\alpha$. The 4th moment is important for the energy difference of the *fcc* and *bcc* structure of the transition metals.

Moments are well known in statistical mathematics as a concept to describe a distribution (in our case the local DOS). The first few moments are often discussed as measures of specific properties of the distribution,

$$\mu_{i\alpha}^{(0)} = \int n_{i\alpha}(E) dE : \text{norm}, \quad (30)$$

$$\mu_{i\alpha}^{(1)} = \int E n_{i\alpha}(E) dE : \text{centre of gravity}, \quad (31)$$

$$\mu_{i\alpha}^{(2)} = \int E^2 n_{i\alpha}(E) dE : \text{root mean square width}, \quad (32)$$

$$\mu_{i\alpha}^{(3)} = \int E^3 n_{i\alpha}(E) dE : \text{skewness}, \quad (33)$$

$$\mu_{i\alpha}^{(4)} = \int E^4 n_{i\alpha}(E) dE : \text{bimodality}. \quad (34)$$

While $\mu_{i\alpha}^{(0)}$ and $\mu_{i\alpha}^{(1)}$ do not contain any information of the surroundings of an atom, the second moment $\mu_{i\alpha}^{(2)}$ is the lowest moment that contains physical information of the environment of an atom (the root mean square width of the density of states). The Hamiltonian is typically attractive, therefore the third moment is typically negative

$$\mu_{i\alpha}^{(3)} = \sum_{j\beta k\gamma} \langle i\alpha | \hat{H} | j\beta \rangle \langle j\beta | \hat{H} | k\gamma \rangle \langle k\gamma | \hat{H} | i\alpha \rangle < 0, \quad (35)$$

and gives rise to a skewed DOS as illustrated in Fig. 3(a). Therefore, if one calculates the energy difference of two densities of states at identical second moment but with $\mu_{i\alpha}^{(3)} = 0$ and $\mu_{i\alpha}^{(3)} < 0$, one obtains as a function of band filling a figure similar to Fig. 3(b). For less than half-full band the negative 3rd moment contribution tends to stabilise the DOS with $\mu_{i\alpha}^{(3)} < 0$ relative to the DOS with vanishing third moment. The third moment gives a first

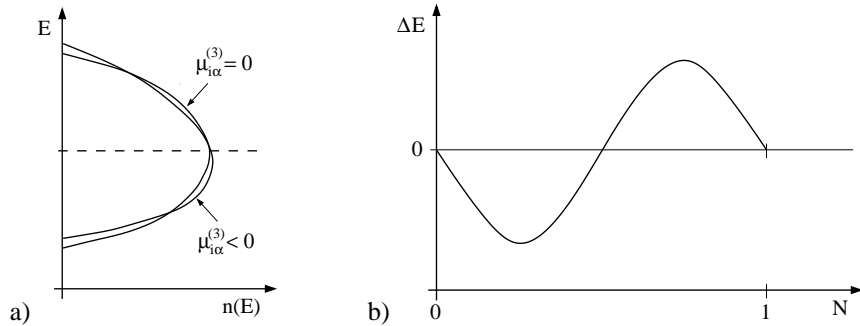


Figure 3. The 3rd moment gives rise to a skewing of the DOS (a) that typically (for $\mu_{i\alpha}^{(3)} < 0$) stabilises close-packed structures for less than half-full band (b).

indication of the crystal structure of elements with less than half-full band (like Mg and Al): the observed close-packed structure offers many self-returning paths of length three and therefore has a large third moment. In contrast, elements with more than half-full band (like Cl and S) tend to avoid a large third moment and therefore form open structures or molecules that have no hopping paths of length three.

The fourth moment characterises the bi-modal (in contrast to uni-modal) behaviour of the density of states as shown in Fig. 4(a). A bimodal DOS has a low density of states at the centre of the band and tends to be stable over a unimodal DOS at half-full band as shown in Fig. 4(b). This is the reason why *sp*-valent elements with half-full band (such as Si, Ge) have a tendency to crystallise in the diamond structure. The discussion of the first four moments may be generalised for higher moments. For example, six moments are required to resolve the energy difference between the close-packed *fcc* and *hcp* lattices¹⁴, many of the small differences between more complex crystal structures can also be resolved with an expansion to only about the 6th moment^{15, 16}. Furthermore, if two structures are different only at the level of the *N*th moment and this *N*th moment dominates, then the energy difference between the two structures shows *N* – 2 zeros between empty and full band¹⁷.

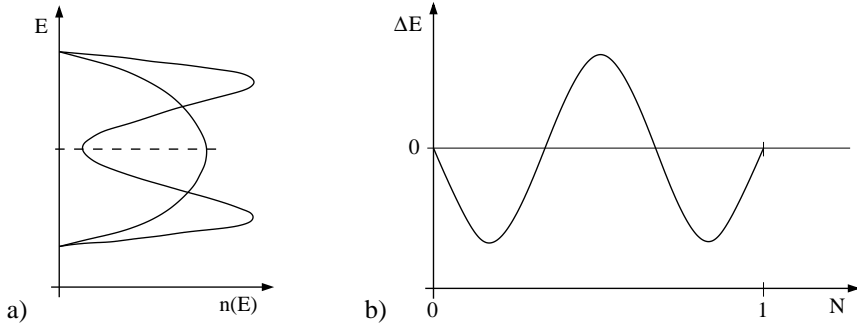


Figure 4. The 4th moment causes the DOS to take a bimodal shape (a), thereby favouring the diamond structure at half-full band.

5 Recursion

In the previous section we showed that the moments of the density of states relate the atomic structure to the electronic structure. A mathematically equivalent way of relating the electronic structure to the crystal structure is the recursion method¹⁸.

Given a starting state $|u_0\rangle$, which we may think of for example as an atomic orbital $|i\alpha\rangle$, the Hamilton operator is used to generate a new state $|u_1\rangle$ by

$$b_1|u_1\rangle = (\hat{H} - a_0)|u_0\rangle. \quad (36)$$

The new state is normalized ($\langle u_1|u_1\rangle = 1$) and orthogonal to $|u_0\rangle$ ($\langle u_1|u_0\rangle = 0$). The coefficients a_0 and b_1 are determined by multiplying from the left with $|u_1\rangle$ and $|u_0\rangle$:

$$b_1 = \langle u_1|\hat{H}|u_0\rangle, \quad (37)$$

$$a_0 = \langle u_0|\hat{H}|u_0\rangle. \quad (38)$$

In a similar fashion, the Hamiltonian is used to generate from $|u_1\rangle$ an other new state $|u_2\rangle$ that cannot be written as a linear combination of $|u_0\rangle$ and $|u_1\rangle$:

$$b_2|u_2\rangle = (\hat{H} - a_1)|u_1\rangle - b_1|u_0\rangle, \quad (39)$$

which is again normalized ($\langle u_2|u_2\rangle = 1$) and orthogonal to $|u_1\rangle$ ($\langle u_2|u_1\rangle = 0$). The coefficients a_1 and b_2 are given correspondingly by

$$b_2 = \langle u_2|\hat{H}|u_1\rangle, \quad (40)$$

$$a_1 = \langle u_1|\hat{H}|u_1\rangle. \quad (41)$$

The general form of the recursion may be written as

$$b_{n+1}|u_{n+1}\rangle = (\hat{H} - a_n)|u_n\rangle - b_n|u_{n-1}\rangle, \quad (42)$$

with the matrix elements

$$b_n = \langle u_n|\hat{H}|u_{n-1}\rangle, \quad (43)$$

$$a_n = \langle u_n|\hat{H}|u_n\rangle. \quad (44)$$

The states $|u_n\rangle$ are orthogonal, $\langle u_n|u_m\rangle = \delta_{nm}$. This means that in the basis $\{|u_0\rangle, |u_1\rangle, |u_2\rangle, \dots\}$, which is generated from the atomic-like orbitals $|u_0\rangle = |i\alpha\rangle$ by recursion, the Hamiltonian matrix takes the following, tridiagonal form

$$\langle u_n | \hat{H} | u_m \rangle = \begin{pmatrix} a_0 & b_1 & & & & \\ b_1 & a_1 & b_2 & & & \\ & b_2 & a_2 & b_3 & & \\ & & b_3 & a_3 & b_4 & \\ & & & b_4 & a_4 & \ddots \\ & & & & \ddots & \ddots \\ & & & & & \ddots \end{pmatrix}.$$

All elements that are not in the diagonal or next to the diagonal are identical to zero. This Hamiltonian matrix may be thought of as the Hamiltonian of a one-dimensional chain with only nearest neighbour hopping matrix elements, see Fig. 5. Using the recursion

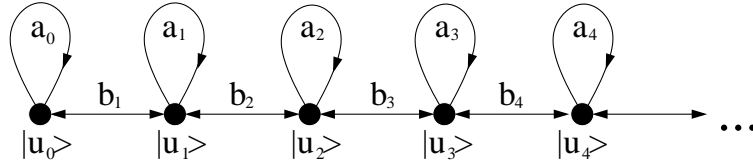


Figure 5. Graphical representation of the recursion Hamiltonian as one-dimensional chain: the Lanczos chain.

and writing $|u_n\rangle$ as linear combination of atomic orbitals, the moments are related to the expansion coefficients a_n and b_n . The N th moment can be determined by summing over all possible paths of length N that start and end on orbital $|u_0\rangle$. For example, the first four moments are given by

$$\mu_{i\alpha}^{(0)} = 1, \quad (45)$$

$$\mu_{i\alpha}^{(1)} = a_0, \quad (46)$$

$$\mu_{i\alpha}^{(2)} = a_0^2 + b_1^2, \quad (47)$$

$$\mu_{i\alpha}^{(3)} = a_0^3 + 2a_0b_1^2 + a_1b_1^2, \quad (48)$$

which is easily verified by identifying all paths of corresponding length in Fig. 5. The purpose of introducing the recursion method in the context of bond-order potentials is to transform the TB Hamiltonian to an orthogonal basis where it takes a tridiagonal form. This procedure of transforming the Hamiltonian to a semi-infinite one-dimensional nearest-neighbour chain is the Lanczos algorithm¹⁹ and establishes an $\mathcal{O}(N)$ approach to calculate the local electronic density of states as we shall see in the following.

6 Green's Functions

In the previous section we learned how to calculate the moments of the density of states from the crystal structure. We would like to use the information contained in the moments

to calculate the bond energy U_{bond} , Eq.(4). The Green's function \hat{G} is closely related to the density of states Eq.(8) and the density matrix Eq.(14), as we will see in the following. It will therefore be helpful for the construction of the bond energy U_{bond} , Eqs.(4) and (15). As a first step in this direction we will use the Green's functions to reconstruct the local density of states $n_{i\alpha}(E)$ from the moments. Once we have obtained the local density of states, we can integrate it to calculate the bond energy. We define the Green's function \hat{G} as the inverse of the Hamiltonian,

$$\hat{G} = (E\hat{1} - \hat{H})^{-1}. \quad (49)$$

As the Hamilton operator in the basis of the eigenstates ψ_n is written as

$$\langle \psi_n | (E\hat{1} - \hat{H}) | \psi_m \rangle = (E_n - E) \delta_{nm}, \quad (50)$$

and by definition of \hat{G} ,

$$\langle \psi_n | (E\hat{1} - \hat{H}) \hat{G} | \psi_m \rangle = \langle \psi_n | \psi_m \rangle = \delta_{nm}, \quad (51)$$

the Green's function matrix elements of the eigenstates may be written explicitly as

$$\langle \psi_n | \hat{G} | \psi_m \rangle = \frac{\delta_{nm}}{E - E_n}. \quad (52)$$

This can be verified by inserting the identity $\hat{1} = \sum_k |\psi_k\rangle\langle\psi_k|$,

$$\langle \psi_n | (E\hat{1} - \hat{H}) \hat{G} | \psi_m \rangle = \sum_k \langle \psi_n | (E\hat{1} - \hat{H}) | \psi_k \rangle \langle \psi_k | \hat{G} | \psi_m \rangle \quad (53)$$

$$= \sum_k (E - E_n) \delta_{nk} \frac{\delta_{km}}{E - E_m} \quad (54)$$

$$= (E - E_n) \delta_{nm} \frac{1}{E - E_m} \quad (55)$$

$$= \delta_{nm}. \quad (56)$$

The matrix elements of the Green's function in the atomic orbital basis $G_{i\alpha j\beta}(E) = \langle i\alpha | \hat{G} | j\beta \rangle$ are obtained as

$$G_{i\alpha j\beta}(E) = \sum_{nm} \langle i\alpha | \psi_n \rangle \langle \psi_n | \hat{G} | \psi_m \rangle \langle \psi_m | j\beta \rangle = \sum_n \frac{c_{i\alpha}^{*(n)} c_{j\beta}^{(n)}}{E - E_n}, \quad (57)$$

By making use of the identity/residue

$$-\frac{1}{\pi} \text{Im} \int \frac{1}{E - E_n} dE = \int \delta(E - E_n) dE, \quad (58)$$

we can replace Eq.(8) and Eq.(14) using matrix elements of the Green's function

$$n_{i\alpha}(E) = -\frac{1}{\pi} \text{Im} G_{i\alpha i\alpha}(E), \quad (59)$$

$$\rho_{i\alpha j\beta} = -\frac{1}{\pi} \text{Im} \int_{E_F}^{E_F} G_{i\alpha j\beta} dE. \quad (60)$$

Connection can now be made to the recursion method introduced in the previous section. The diagonal element of the Green's function at the starting orbital of the semi-infinite one-dimensional Lanczos chain is given as a continued fraction²⁰

$$G_{i\alpha i\alpha} = G_{00} = \frac{1}{E - a_0 - \frac{b_1^2}{E - a_1 - \frac{b_2^2}{E - a_2 - \frac{b_3^2}{\ddots}}}}. \quad (61)$$

The continued fraction expansion provides a direct way of calculating the density of states which in turn may be used to calculate the bond energy.

Taking the continued fraction to an infinite number of recursion levels corresponds to an exact solution of the tight-binding model. By *terminating* the continued fraction after a certain number of levels, a local expansion of the electronic structure is obtained. The different flavors of using truncated Green's function expansion for a local calculation of the bond energy are presented in the following section. A more detailed review of the connection between bond-order potentials, Green's functions and the recursion method is given, *e.g.*, in Refs. 21–23.

7 Calculation of the Bond-Energy I – Numerical Bond-Order Potentials

The recursion expansion representation of the Hamiltonian Eq. (42) offers a direct way of writing the onsite Greens-function matrix elements $G_{i\alpha i\alpha} = \langle i\alpha | \hat{G} | i\alpha \rangle = G_{00}$ in the form of a continued fraction expansion, Eq.(61). For the bond-order potentials we are interested in a local calculation of the bond energy and not in an exact solution of the underlying TB model. This is achieved by *terminating* the expansion after a few recursion levels n . This is equivalent to evaluating the first $2n + 1$ moments of the density of states (cf. Sec. 5). In the simplest case, the recursion coefficients a_m and b_m for $m > n$ are replaced by a constant terminator

$$a_m = a_\infty, \quad b_m = b_\infty \quad \text{for } m > n. \quad (62)$$

By inserting the continued fraction expression for the Green's function matrix element Eq.(61) in Eq.(59) one obtains an approximate closed-form representation of the density of states $n_{i\alpha}$. The bond energy Eq.(4) is obtained by *numerical* integration of

$$U_{\text{bond}} = -\frac{2}{\pi} \text{Im} \int_{E_F}^{\infty} (E - E_{i\alpha}) \frac{1}{E - a_0 - \frac{b_1^2}{E - a_1 - \frac{\ddots}{E - a_\infty - \frac{b_\infty^2}{E - \ddots}}}} dE \quad (63)$$

and therefore this representation of the energy is called numerical bond-order potential. In general the approximation error in the bond energy will become smaller with more

recursion levels n taken into account exactly. Therefore, the number of recursion levels provides a way of systematically converging the bond energy to the bond energy that one obtains from an exact solution of the TB Hamiltonian.

For the calculation of the forces on the atoms one requires the bond-order/density matrix and therefore the calculation of $G_{i\alpha j\beta}$. For numerical stability and convergence of the continued fraction expansion of $G_{i\alpha j\beta}$, one relates $G_{i\alpha j\beta}$ to the onsite matrix elements $G_{i\alpha i\alpha}$ and $G_{j\beta j\beta}$. This is achieved by using a linear combination of atomic orbitals in the recursion expansion

$$|u_0\rangle = \frac{1}{\sqrt{2}} (|i\alpha\rangle + e^{i\vartheta} |j\beta\rangle) , \quad (64)$$

with $\vartheta = \cos(\lambda)$ such that

$$G_{00} = \lambda G_{i\alpha j\beta} + \frac{1}{2} (G_{i\alpha i\alpha} + G_{j\beta j\beta}) . \quad (65)$$

Therefore, the intersite matrix elements of the Green's function is given as a derivative of the onsite elements of the starting Lanczos orbital, a central result of BOP theory²⁴

$$G_{i\alpha j\beta} = \left. \frac{d}{d\lambda} G_{00} \right|_{\lambda=0} . \quad (66)$$

At any level of approximation exists a termination of the expansion of $G_{i\alpha j\beta}$ which ensures that the onsite and intersite representation of the bond energy are identical²⁵, as of course it would have to be if the problem would have been solved exactly. A detailed review of the numerical bond-order potentials is available in Ref. 5.

8 Calculation of the Bond-Energy II – Analytic Bond-Order Potentials

As the integral for the calculation of the bond energy in Eq.(63) is carried out numerically in numerical BOPs, no analytic representation of the effective interactions between atoms and therefore no analytic interatomic potential may be obtained. In this section we will discuss how analytic representations of the bond energy may be obtained, such that explicit analytic interatomic potentials may be written down.

8.1 Analytic Bond-Order Potentials for Semiconductors

If the expansion of $G_{i\alpha i\alpha}$ in Eq.(61) is terminated with $a_\infty = 0$ and $b_\infty = 0$ after only two recursion levels ($n = 2$) corresponding to four moments, the integral for the bond energy Eq.(63) may be carried out analytically. In order to achieve a good convergence with only two recursion levels, the starting state of the recursion $|u_0\rangle$ must be taken as an as close approximation of the solution as possible. For semiconductors with saturated covalent bonds one achieves very good convergence if the starting state is chosen as a dimer orbital^{26,27}

$$|u_0\rangle = \frac{1}{\sqrt{2}} (|i\alpha\rangle + |j\beta\rangle) . \quad (67)$$

The resulting analytic bond-order potentials^{26,27} have been applied to modelling the growth of semiconductor films and hydrocarbons. A detailed review of the analytic BOPs for semiconductors may be found in Refs. 6,7. If one takes the expansion of this analytic bond-order potential only to two moments of the density of states instead of four moments, then an expansion is obtained that is very close²⁸ to the empirical potential given by Tersoff²⁹. Therefore the analytic BOP may be viewed as an systematic extension of the Tersoff-Brenner-type potentials.

8.2 Analytic Bond-Order Potentials for Transition Metals

In a close-packed transition metal, the bonds between atoms are not saturated. Therefore the expansion of the analytic BOPs for semiconductors that is built on a saturated dimer bond may not be directly applied to transition metals. Instead of taking a dimer orbital as the starting state of the expansion, inserting a spherical atomic orbital into a close-packed crystal structure leads to a faster convergence of the expansion. However, in order to resolve for example the energy difference between the *fcc* and *hcp* structure in a canonical TB model³⁰, at least six moments are required¹⁴. For six moments or equivalently three recursion levels, the integration of Eq.(63) cannot be carried out analytically. Instead of integrating Eq.(63), one therefore constructs a perturbation expansion of the continued fraction representation of $G_{i\alpha i\alpha}$. This perturbation expansion may then be integrated analytically.

The starting point of the expansion is the observation that the Green's function may be written down in a compact form if all the expansion coefficients a_n and b_n are taken identical to

$$a_n = a_\infty \quad , \quad (68)$$

$$b_n = b_\infty \quad . \quad (69)$$

Then the density of states is given by

$$n_{i\alpha}^{(0)}(\varepsilon) = \frac{2}{\pi} \sqrt{1 - \varepsilon^2}, \quad (70)$$

with the normalized energy ε ,

$$\varepsilon = \frac{E - a_\infty}{2b_\infty} \quad . \quad (71)$$

The density of states $n_{i\alpha}^{(0)}(\varepsilon)$ is then used as the reference density of states in a perturbation expansion³¹

$$n_{i\alpha}(\varepsilon) = n_{i\alpha}^{(0)}(\varepsilon) + \delta n_{i\alpha}(\varepsilon). \quad (72)$$

Chebyshev polynomials $P_n(\varepsilon)$ of the second kind are orthogonal with respect to the weight function $n_{i\alpha}^{(0)}$,

$$\frac{2}{\pi} \int_{-1}^{+1} P_n(\varepsilon) P_m(\varepsilon) \sqrt{1 - \varepsilon^2} d\varepsilon = \delta_{nm}. \quad (73)$$

The density of states is thus expanded in terms of Chebyshev polynomials

$$n_{i\alpha}(\varepsilon) = \frac{2}{\pi} \sqrt{1 - \varepsilon^2} \left(\sigma_0 + \sum_{n=1} \sigma_n P_n(\varepsilon) \right), \quad (74)$$

with expansion coefficients σ_n . The expansion coefficients are related to the moments of the density of states Eq.(29) by writing the Chebyshev polynomials explicitly in the form of polynomials with coefficients p_{mk} ,

$$P_m(\varepsilon) = \sum_{k=0}^m p_{mk} \varepsilon^k. \quad (75)$$

Then the expansion coefficients σ_m are obtained in terms of the moments $\mu_{i\alpha}^{(k)}$,

$$\sigma_m = \int_{-1}^{+1} \sum_{k=0}^m p_{mk} \varepsilon^k n_{i\alpha}(\varepsilon) d\varepsilon = \sum_{k=0}^m p_{mk} \int_{-1}^{+1} \varepsilon^k n_{i\alpha}(\varepsilon) d\varepsilon = \sum_{k=0}^m p_{mk} \hat{\mu}_{i\alpha}^{(k)}, \quad (76)$$

where we introduced the normalized moments

$$\hat{\mu}_{i\alpha}^{(n)} = \frac{1}{(2b_{i\infty})^n} \sum_{l=0}^n \binom{n}{l} (-a_{i\infty})^{(n-l)} \mu_{i\alpha}^{(l)}. \quad (77)$$

Therefore, by calculating the moments $\mu_{i\alpha}^{(k)}$ according to Eq.(29) by pathcounting and inserting the expansion coefficients σ_n into the expansion Eq.(74), one obtains a closed-form approximation of the density of states. Integration of the density of states analytically yields an analytic expression for the bond energy associated with orbital $i\alpha$

$$U_{\text{bond},i\alpha} = \int_{-1}^{E_F} (E - E_{i\alpha}) n_{i\alpha}(\varepsilon) d\varepsilon = \sum_n \sigma_n [\hat{\chi}_{n+2}(\phi_F) - \gamma \hat{\chi}_{n+1}(\phi_F) + \hat{\chi}_n(\phi_F)], \quad (78)$$

where we introduced the so-called response functions

$$\hat{\chi}_n(\phi_F) = \frac{1}{\pi} \left(\frac{\sin(n+1)\phi_F}{n+1} - \frac{\sin(n-1)\phi_F}{n-1} \right), \quad (79)$$

and the Fermi phase $\phi_F = \cos^{-1}(E_F/2b_{i\infty})$.

The lowest order approximation of the analytic bond-order potential that includes only two moments is similar to the Finnis-Sinclair potential³², so that the analytic BOP expansion may be viewed as a systematic extension of the Finnis-Sinclair potential to include higher moments. On the other hand, as the expression for the bond energy may be integrated analytically for an arbitrary number of moments, the expansion Eq.(78) provides an effective interatomic interaction that may be systematically converged with respect to the exact solution of the TB Hamiltonian by including higher moments. As in the case of the numerical bond-order potentials, the bond energy, Eq.(78), may be rewritten as an equivalent intersite representation. A detailed derivation of the analytic bond-order potentials for transition metals may be found in Ref. 14.

9 Calculation of Forces

The computationally fast and efficient calculation of forces is important for efficient molecular dynamics simulations. In self-consistent electronic structure calculations the Hellmann-Feynman theorem^{33,34} makes an efficient calculation of forces possible, as only gradients of the Hamiltonian matrix elements need to be evaluated. The contribution of the bond energy to the forces may be written as

$$\mathbf{F}_k = \nabla_k U_{bond} = \sum_{i\alpha \neq j\beta} \Theta_{i\alpha j\beta} \nabla_k H_{j\beta i\alpha}. \quad (80)$$

The Hamiltonian matrix elements are pairwise functions, therefore the calculation of the gradients is very efficient. For the bond-order potentials Hellmann-Feynman-like forces¹⁴ may be derived that may be written in a form similar to the Hellmann-Feynman forces Eq.(80),

$$\mathbf{F}_k = \nabla_k U_{bond} = \sum_{i\alpha \neq j\beta} \tilde{\Theta}_{i\alpha j\beta} \nabla_k H_{j\beta i\alpha}, \quad (81)$$

where $\tilde{\Theta}_{i\alpha j\beta}$ is an approximate representation of the bond order. Just as in the case of the Hellmann-Feynman forces, the calculation of the forces in the bond-order potentials requires only the calculation of the gradient $\nabla_k H_{j\beta i\alpha}$ and not the differentiation of a complex many-body function and is therefore computationally efficient compared to the evaluation of the gradient of an empirical many-body potential.

10 Conclusions

This introductory lecture provides a brief guide to the central ideas and concepts behind the derivation of the bond-order potentials. Instead of diagonalising the TB Hamiltonian, the bond-order potentials provide an approximate local solution of the TB Hamiltonian and the binding energy. The local solution is constructed as a function of the crystal structure or, more general, the positions of the atoms, by relating the electronic structure to the crystal structure using the moments theorem. In this way explicit parametrisations of the energy as a function of the atomic positions are obtained. The accuracy of the bond-order potential with respect to the corresponding tight-binding solution can be improved systematically by including higher moments, which corresponds to taking into account more far-sighted atomic interactions. Hellmann-Feynman-like forces allow for an efficient calculation of the forces in molecular dynamics simulations.

Acknowledgements

We are grateful to D.G. Pettifor for a critical reading of the manuscript. We acknowledge EPSRC funding for part of our work in the projects *Alloy by Design: A materials modelling approach* and *Mechanical Properties of Materials for Fusion Power Plants*.

References

1. A.T. Paxton, *An introduction to the tight binding approximation - implementation by diagonalisation*, in this volume
2. A.P. Sutton, M.W. Finnis, D.G. Pettifor, and Y. Ohta, *The tight-binding bond model*, J. Phys. C **21**, 35, 1988
3. *Modelling electrons and atoms for materials science*, edited by M.W. Finnis and R. Drautz, Prog. Mat. Sci. **52**, Issues 2-3, 2007
4. M.W. Finnis, *Bond-order potentials through the ages*, Prog. Mat. Sci. **52**, 133, 2007
5. M. Aoki, D. Nguyen-Manh, D.G. Pettifor, and V. Vitek, *Atom-based bond-order potentials for modelling mechanical properties of metals*, Prog. Mat. Sci. **52**, 154, 2007
6. R. Drautz, X.W. Zhou, D.A. Murdick, B. Gillespie, H.N.G. Wadley and D.G. Pettifor, *Analytic bond-order potentials for modelling the growth of semiconductor thin films*, Prog. Mat. Sci. **52**, 196, 2007
7. M. Mrovec, M. Moseler, C. Elsässer, and P. Gumbsch, *Atomistic modeling of hydrocarbon systems using analytic bond-order potentials*, Prog. Mat. Sci. **52**, 230, 2007
8. M. Mrovec, D. Nguyen-Manh, D.G. Pettifor, and V. Vitek, *Bond-order potential for molybdenum: Application to dislocation behaviour*, Phys. Rev. B **69**, 094115, 2004
9. D.G. Pettifor, *The tight-binding bond model*, Commun. Phys. (London) **1**, 141, 1976
10. A.R. Mackintosh and O.K. Andersen, Chap. 5.3, *Electrons at the Fermi surface*, (Cambridge University Press, 1980)
11. R. Drautz, D.A. Murdick, D. Nguyen-Manh, X.W. Zhou, H.N.G. Wadley, and D.G. Pettifor, *Analytic bond-order potential for predicting structural trends across the sp-valent elements* Phys. Rev. B **72**, 144105, 2005
12. D.G. Pettifor, *Bonding and Structure of Molecules and Solids* (Oxford University Press, Oxford, 1995)
13. F. Cyrot-Lackmann, *On the electronic structure of liquid transition metals*, Adv. Phys. **16**, 393, 1967
14. R. Drautz and D.G. Pettifor, *Valence-dependent analytic bond-order potential for transition metals*, Phys. Rev. B **74**, 174117, 2006
15. P.E.A. Turchi, *Interplay between local environment effect and electronic structure properties in close packed structures*, Mat. Res. Soc. Symp. Proc. **206**, 265, 1991
16. T. Hammerschmidt, B. Seiser, R. Drautz, and D.G. Pettifor, *Modelling topologically close-packed phases in superalloys: Valence-dependent bond-order potentials based on ab-initio calculations*, in: *Superalloys 2008*, edited by R. C. Reed (The Metals, Minerals and Materials Society, Warrendale, 2008), p. 0487
17. F. Ducastelle and F. Cyrot-Lackmann, *Moments developments- II. Application to the crystalline structures and the stacking fault energies of transition metals* J. Phys. Chem. Solids **32**, 285, 1971
18. R. Haydock, *Recursive solution of the Schrödinger equation*, Comp. Phys. Comm. **20**, 11, 1980
19. C. Lanczos, *An iteration method for the solution of the eigenvalue problem of linear differential and integral operators*, J. Res. Natl. Bur. Stand. **45**, 225, 1950
20. R. Haydock, V. Heine, and M.J. Kelly, *Electronic structure based on the local atomic environment for tight-binding bands*, J. Phys. C: Sol. Stat. Phys. **5**, 2845, 1972

21. D.G. Pettifor, *New many-body potential for the bond-order*, Phys. Rev. B **63**, 2480, 1989
22. A. Horsfield, A.M. Bratkovsky, M. Fearn, D.G. Pettifor, and M. Aoki, *Bond-order potentials: Theory and implementation*, Phys. Rev. B **53**, 12694, 1996
23. M. W. Finnis, *Interatomic forces in condensed matter* (Oxford University Press, Oxford, 2007)
24. M. Aoki, and D.G. Pettifor, in *International Conference on the Physics of Transition Metals: Darmstadt, Germany, July 2024, 1992*, edited by P. M. Oppeneer and J. K. Kübler (World Scientific, Singapore, 1993), p. 299
25. M. Aoki, *Rapidly convergent bond order expansion for atomistic simulations*, Phys. Rev. Lett. **71**, 3842, 1993
26. D.G. Pettifor, and I.I. Oleinik, *Bounded Analytic Bond-Order Potentials for σ and π Bonds*, Phys. Rev. Lett. **84**, 4124, 2000
27. D.G. Pettifor, and I.I. Oleinik, *Analytic bond-order potentials beyond Tersoff-Brenner. I. Theory*, Phys. Rev. B **59**, 8487, 1999
28. P. Alinaghian, P. Gumbsch, A.J. Skinner, and D.G. Pettifor, *Bond order potentials: a study of s- and sp-valent systems*, J. Phys.: Cond. Mat. **5**, 5795, 1993
29. J. Tersoff, *New empirical model for the structural properties of silicon*, Phys. Rev. Lett. **56**, 632, 1986
30. O.K. Andersen, W. Klose, and H. Nohl, *Electronic structure of Chevrel-phase high-critical-field superconductors*, Phys. Rev. B **17**, 1209, 1978
31. R. Haydock, *Recursive solution of Schrödinger's equation*, Sol. Stat. Phys. **35**, 215, 1980
32. M.W. Finnis, and J.E. Sinclair, *A simple empirical n-body potential for transition metals*, Phil. Mag. A **50**, 45, 1984
33. H. Hellmann, in: *Einführung in die Quantenchemie*, (Deuticke, Leipzig, 1937)
34. R.P. Feynman, *Forces in molecules*, Phys. Rev. **56**, 340, 1939